The Characteristic Spatial and Temporal Scales for SLP, SST, and Air Temperature in the Southern Hemisphere

JOHN COLOSI AND TIM P. BARNETT

Scripps Institution of Oceanography, La Jolla, California

(Manuscript received 9 December 1988, in final form 22 January 1990)

ABSTRACT

This study summarizes results of an analysis of the TOGA drifting buoy observations in the Southern Hemisphere. The data were first quality controlled for gross errors and then screened against climatology and products from national weather centers. The characteristic space scales of the SLP, SST, and air temperature fields for the summer months of December, January, and February, and the winter months of June, July, and August were determined next. Typical decorrelation distances for all fields were between 1200–2800 km with the correlations being generally isotropic. This information suggests that roughly 30–40 fully functional buoys evenly distributed over the southern oceans from 15° to 60°S should be able to resolve the major scales of Southern Hemisphere climate change.

1. Introduction

Conventional atmospheric and oceanic data obtained by ship reports, air flights, etc., are predominantly concentrated over main commercial shipping routes and there are huge regions of the Southern Hemisphere oceans where data coverage is insufficient to define climatic changes. As a result of this biased data sampling, the TOGA (Tropical Ocean Global Atmosphere) program has supported a drifting buoy program in the Southern Hemisphere, with the goal of providing observations of sea level pressure (SLP), sea surface temperature (SST), and air temperature (T) from the infrequently traveled regions in the southern oceans. The aim of this effort was to fill data-sparse areas and so improve meteorological and oceanographic products routinely produced by operational centers (e.g., the National Meteorological Center (NMC), Australian Bureau of Meteorology, etc.). The drifting buoy program became operational in 1984 and data soon began to flow to the various operational centers. Preliminary studies of the impact such increased observation density had on GCM predictive ability were very encouraging.

Against the background of this success is the fact that the TOGA drifting buoy data have been exploited little to date by the scientific community as a self-contained dataset. This paper, then, describes the TOGA drifter data, some of their problems and then compares the data with conventional measurements to establish how reasonable it is. Another goal of this paper is to extract from the TOGA drifter data relevant information concerning deployment schemes for Southern Hemisphere drifters. In this way an observational array may be designed such that maximum information can be extracted from the ocean/atmosphere system with minimum cost. To this end a two dimensional correlation analysis was conducted to estimate the decorrelation length scales of the SLP, SST, and T fields. The results of this analysis will then give us estimates of the characteristic scale lengths of the SLP, SST, and T fields and these may be used to determine roughly the number of drifters required to monitor those fields.

Section 2 describes the necessary editing of the TOGA drifter data and geographic distribution of buoy observations during the period 1 November 1984 to 31 December 1986. In addition section 2 compares the drifter data with standard ocean and atmosphere products. In section 3 a discussion of the correlation analysis is advanced. The decorrelation distances obtained from the two-dimensional correlation analysis for the South Pacific and the South Atlantic are also presented. Section 4 contains a summary of this study.

2. Data

a. Data processing and intercomparison

TOGA drifting buoy data obtained between 1 November 1984 to 31 December 1986 was provided courtesy of Wilbur Biggs of the National Climatic Data Center in Asheville, North Carolina. These data were initially collected via satellite from the French system ARGOS and transmitted over the GTS (Global Telecommunications System) circuit in near real time. The data were taken from the GTS circuit by the National

Corresponding author address: John Colosi, Physics Department, University of California at Santa Cruz, Santa Cruz, CA 95064.

Data Buoy Center (NDBC) where it was lightly quality controlled and reformatted. In spite of the quality control that was conducted at the NDBC, the TOGA drifter data required quite a lot of editing to make it usable. NDBC has since been given a stronger quality control responsibility (Hamilton personal communication) and that will hopefully make the buoy data more amenable to scientific use. Indeed, recent work by Gilhousen (1987) documents buoy problems and quality control strategies to cure them.

The editing of the raw TOGA buoy data uncovered three main problems:

1) It became clear immediately that data were being logged before the buoy had been deployed. This conclusion was reached by examining the SST and T records, which in some cases turned out to be almost identical in regard to the magnitude of the daily cycle. This problem was easily cured by retrieving the launch records from the NDBC. It should be noted that a few of the buoys were launched then picked up and launched again. They reported data continuously; whether freely drifting in the ocean, on shipboard, or in the middle of Madagascar awaiting deployment.

2) Another problem that was obvious from the start was the occurrence of erroneous observations in the records due to problems in data transmission, data processing, or the like. Examples of this were SSTs that were near 45°C, SLPs that dipped below 900 mb, latitudes or longitudes that had the wrong sign, or simply random spikes in the data. These problems were resolved by comparisons with existing climatologies (automated) and visual inspection.

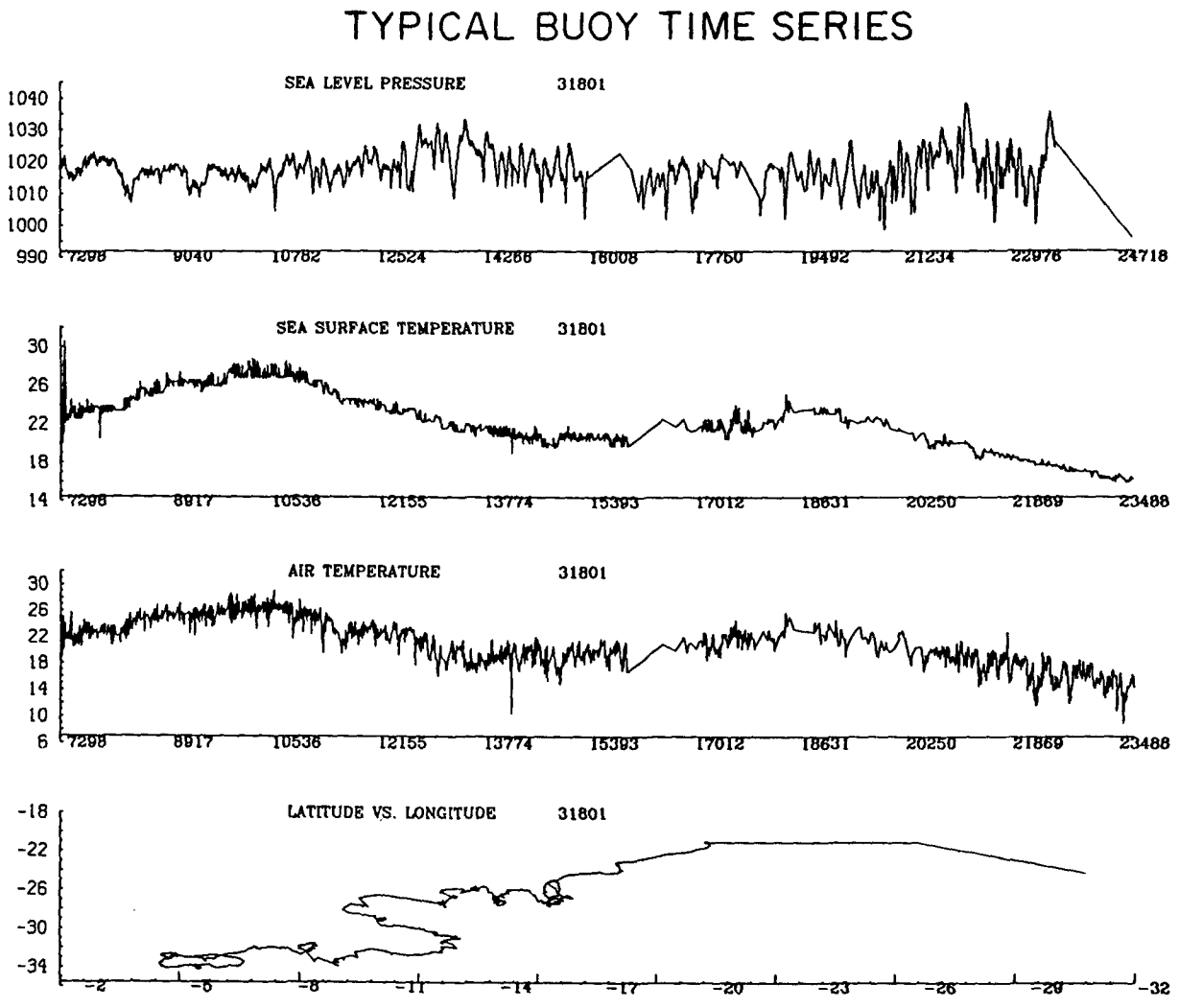

FIG. 1. Data for Buoy number 31801 deployed in the South Atlantic. The upper three panels give the time evolution of the observed SLP (mb), SST (°C), and T (°C) fields, respectively. Time is measured in hours. The lower panel gives the buoy trajectory where latitude (degrees south) is on the Y axis and longitude (degrees west) is on the X axis. The straight lines in the record are times when there is no data.

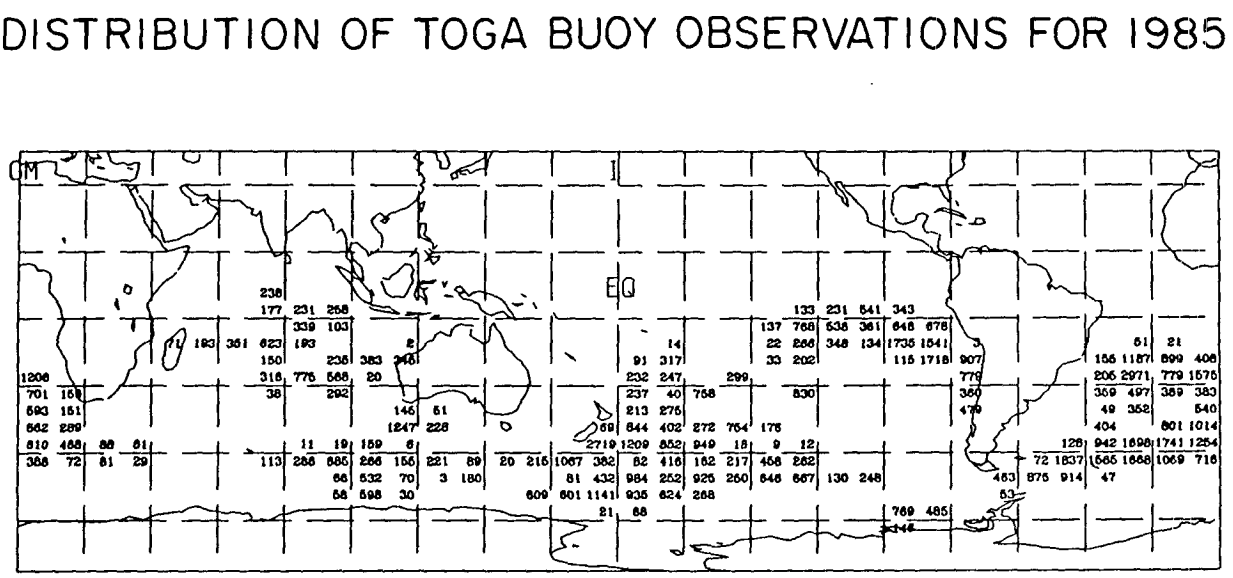

FIG. 2. Geographical distribution of TOGA drifter observations for 1985. Displayed values represent the number of individual reports that fell in boxes of 5° lat × 10° long.

3) The final problem to be overcome was a difficulty in the latitudes and longitudes that stemmed from a reformatting error at the NDBC. From the inception of the TOGA drifter program to 6 September 1985, the NDBC was processing the system ARGOS data with the belief that the lat/longs were actually in hundredths of a degree when in fact they were expressed in degrees and minutes.

The data that passed the quality control filters amounted to 90.73% of the original data volume. Figure 1 displays typical edited data for a selected buoy. The geographic coverage of the TOGA buoys for the years 1985 and 1986, respectively, represented by the number of SLP observations in a year for 5° lat × 10° long boxes are shown in Figs. 2 and 3. The coverage for the other variables; i.e., SST and T, were very similar although there were, in general, more SLP observations. Note, also, that more data were collected in 1986 (109 138 observations) than in 1985 (83 379 observations), owing to an increased number of operational buoys.

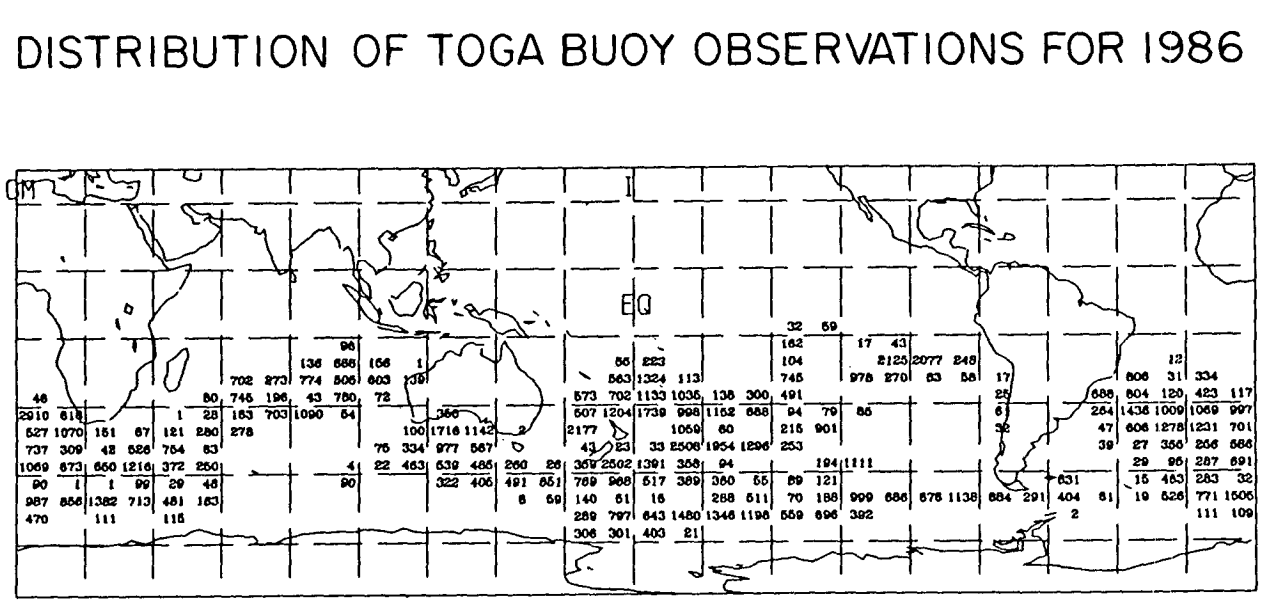

FIG. 3. Geographical distribution of TOGA drifter observations for 1986. Displayed values represent the number of individual reports that fell in boxes of 5° lat × 10° long.

b. Data intercomparisons

The buoy data were compared with three different "standard" datasets; one for SST and two for SLP. The methods and results are as follows:

SST: An updated, although "interim," version of the COADS data were used to obtain monthly SST data on a 4° lat × 4° long grid. If at least 20 buoy observations were available within a given 4 × 4 box in a given month then the average of these values was used to give a "buoy" SST field. Corresponding pairs of monthly averaged buoy and COADS values are shown on a scatter plot in Fig. 4. The agreement is obviously excellent over the range from 28°C to near −2°C and the bias is small. For unexplained reasons the 1986 data show more scatter with maximum individual discrepancies of up to 3°C. However, on balance, the buoys seem to be returning data that is highly complementary to commonly used measures of SST. In fact, we expect that some of the buoy SST data also entered the COADS via the GTS (S. Woodruff, personal communication), but we could not easily determine how much.

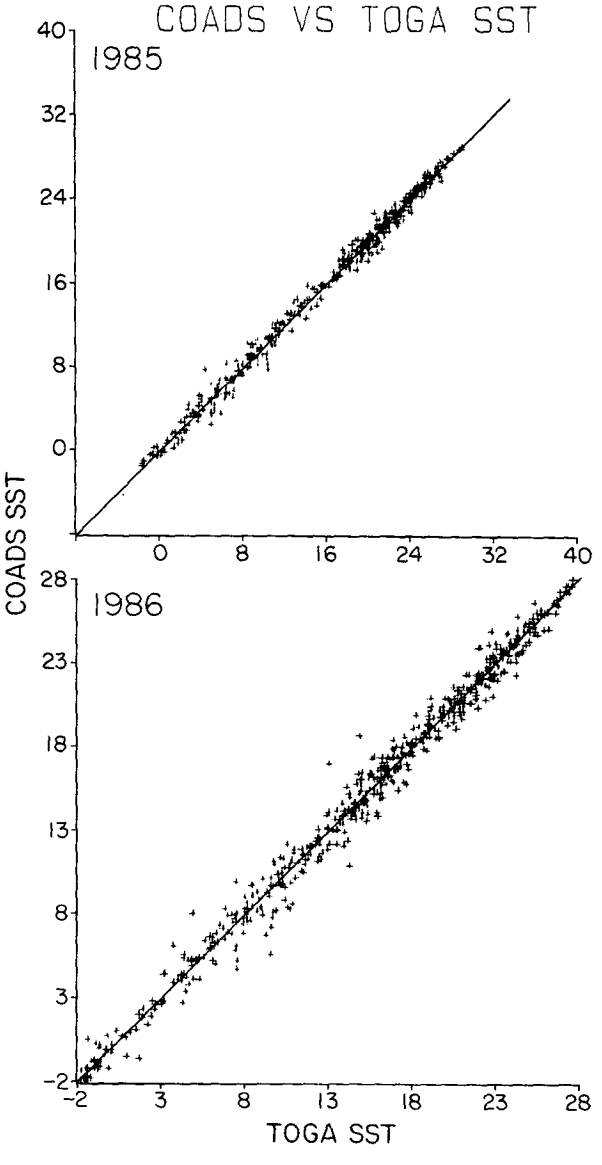

FIG. 4. Comparison of TOGA drifter data with COADS monthly mean SST (°C) records for 1985 and 1986. In 1985 the regression relation had a slope of 1.00 and a y intercept of 0.03°C. In 1986 the slope was 1.00 and a y intercept of 0.01°C.

In some places, therefore, there may be identical data in both datasets, thereby enhancing the agreement in Fig. 4. In any event, the Climate Analysis Center began using buoy data in its blended product in late 1985 (Trenberth and Olson 1988; Reynolds 1988). Given the distribution of observations (Figs. 2 and 3), we can expect that product to be quite representative of SST in the southern oceans, particularly in view of the enhanced quality control that should remove the larger outliers seen in Fig. 4 (Reynolds 1988).

SLP—National Meteorological Center Analysis: The twice daily NMC global analysis was available on a 2.5° × 2.5° grid. These data were averaged to form a monthly mean field. Buoy values of SLP that were within ±2° long and ±1° lat of an NMC grid point were averaged over a month and assigned to the NMC grid point. Monthly values composed of less than 50 individual observations were ignored in subsequent analysis. Scatter diagrams of the corresponding pairs of monthly SLP values for 1985 and 1986 are shown in Fig. 5. The agreement is better in 1985 than 1986 when the scatter is rather large with 10–15 mb differences being common. The *average absolute value* of the difference between NMC and buoy SLP pair values is 2.9 mb in 1985 and 4.0 mb in 1986 (estimated over 655 and 752 pairs, respectively). A separate analysis showed most of the scatter occurred during the southern winter; a result one might expect a priori. Again, we expect a fair amount of buoy data were available for the NMC analyses but we do not know the importance it carried with the final product; apparently not too much. For additional discussion of the NMC products, see Trenberth and Olson (1988).

SLP—Australian Weather Service: The Australian SLP field was available to us on a 5° lat × 10° long grid in monthly averaged format. The daily data were not readily available to us and that may partially affect the results that follow. The monthly average buoy SLP field was formed as described above. The paired values are shown on a scatter plot (Fig. 6). The general agreement is as good as we might expect since at least some of the buoy data went into the analysis. The average absolute difference was 2.0 mb in 1985 and 2.5 mb in 1986. Again, the scatter is larger in 1986 than 1985. But a close inspection shows that some of the largest differences in 1986 are common to both Fig. 5 and Fig. 6. So the analyses agreed with each other but not

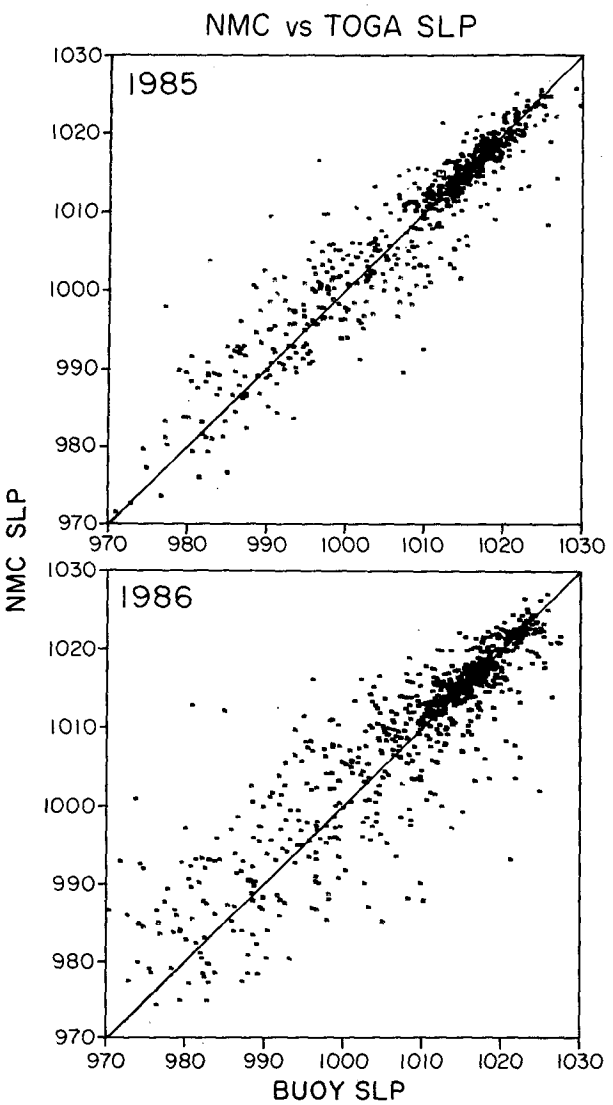

FIG. 5. Comparison of TOGA drifter data with monthly mean SLP (mb) from NMC for 1985 and 1986. In 1985 the regression relation had a slope of 0.87 while in 1986 it was 0.82.

the buoy data. Perhaps our quality control missed some unusual observations; perhaps both analyses were wrong or the results may be influenced by the use of monthly means and the temporal sampling. The discrepancies occurred in winter with the buoy SLPs being lower than the analyses, a situation to be expected if the models missed strong but small storm systems.

In summary, the buoy SST field compares exceedingly well with the extended COADS product. The SLP comparisons are not as good, particularly for the NMC field. It is not clear how strongly the buoy observations weigh into all of the analyses, but one would hope that the analysis schemes could at least have reproduced the observations that went into them. A more complete check would have been to compare the buoy observations with the daily analyses. A case study by Trenberth and Olson 1988 found that the NMC analysis in 1985 took little account of the available observations. This situation improved after 1986.

3. Characteristic length scales

a. Theory

A major goal of this study was to determine the characteristic length scales of the Southern Hemisphere SST, SLP and T fields. We did this in two ways: structure functions (Tatarski 1961), defined as

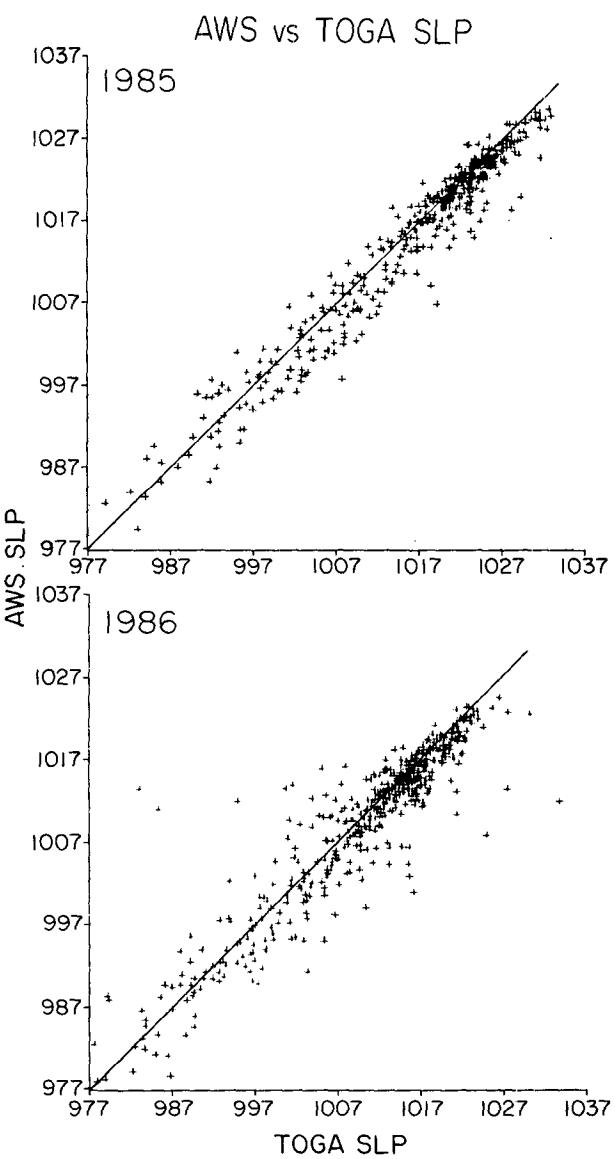

FIG. 6. Comparison of drifter TOGA data with monthly mean SLP (mb) records from the Australian Weather Service for 1985 and 1986. In 1985 the regression relation had a slope of 0.97. In 1986 the slope was 0.89.

$$D(\vec{r}, \tau) = \langle (\eta(\vec{x}, t) - \eta(\vec{x} + \vec{r}, t + \tau))^2 \rangle_{\vec{x},t} \quad (1)$$

were computed for all fields where a specific variable (SST, etc.) is denoted here by η. The absolute position is $\vec{x}$, t is time and $\vec{r}$ and τ the separations in space and time, respectively. We also computed the more conventional spatial correlation functions

$$C(\vec{r}, \tau) = \langle \eta(\vec{x}, t)\eta(\vec{x} + \vec{r}, t + \tau) \rangle_{\vec{x},t}, \quad (2)$$

where $\eta(\vec{x}, t)$ and $\eta(\vec{x} + \vec{r}, t + \tau)$ are fields with zero mean and unit variance. The use of D is desirable when the field being analyzed is only quasi-homogeneous or "piecewise" stationary. In a fully-homogeneous field (Tatarski 1961)

$$D(\vec{r}, \tau) = 2[C(o, o) - C(\vec{r}, \tau)]. \quad (3)$$

Our calculations showed that (3) held roughly for the local data fields under study so we present the results in terms of the more conventional analysis (2).

The above procedure carried out in fields with a strong spatial gradient; e.g., the meridional gradient of SST, will leave the gradient unaltered. The result (2) then will be totally dominated by the mean gradient field. However, we are interested in variability associated with fluctuations in η, not in mean gradient properties, since that is the information necessary for a buoy deployment planning.

The above problem can be largely overcome by using a semi-Eulerian approach. In this case, we compute the means and standard deviations as a function of position and month; e.g.,

$$\bar{\eta} = \langle \eta \rangle_t = \bar{\eta}(\vec{x}) \quad (4)$$

and use these in the equivalent version of (2); i.e.,

$$C(\vec{r}, \tau) = \frac{\langle (\eta(\vec{x}, t) - \bar{\eta}(\vec{x}))(\eta(\vec{x}', t') - \bar{\eta}(\vec{x}')) \rangle_{\vec{x},t}}{\sigma_{\vec{x}}\, \sigma_{\vec{x}'}} \quad (5)$$

where σ are the standard deviations and $\vec{x}' = \vec{x} + \vec{r}$, $t' = t + \tau$.

Note in (5) we have performed an ensemble average of all point pair correlations, effectively removing the $\vec{x}$ dependence normally expected in a purely Eulerian correlation. Given the apparent homogeneity of the η, this should not cause any problem.

There is one problem with the above procedure. From (4), $\bar{\eta}$ and $\sigma(\vec{x})$ are computed over all values of η associated with a particular location. However, due to the inhomogeneities of spatial sampling with time only *some* of the values will enter (5). Thus, the estimation of C via (5) is biased. Fortunately, this problem is minimized by appeal to the Central Limit Theorem and the "Theorem of Large Numbers." Hence the ensemble of a large number of realizations of random variables distributed about different means will have a mean that is the average of the means from the contributing distributions. In our case, each distribution was fixed to have zero mean. As long as enough individual estimates of C are available for averaging, the bias problem will be minimized because the error in the mean goes as $N^{-1/2}$. We computed the bias, $\bar{C}$, for different numbers of independent pairs (N) and found $\bar{C} \leq 0.04$ if $N \geq 2000$. With a few noted exceptions, correlation discussed hereafter had far more than 2000 pairs contributing to the ensemble average (5).

b. *Computational procedure*

The estimates of C were obtained as follows:

1) For winter and summer, regions of the South Pacific and the South Atlantic were selected for correlation analysis on the basis that there was good sampling and adequate coverage of the physically interesting regions of the ocean/atmosphere climate system. The South Pacific summer and winter regions were the same and extended from 20° to 60°S and from 150°E to 150°W. In the Atlantic Ocean, the summer analysis extended from 20° to 60°S and from 40°E to 40°W. In the winter, the analysis extended from 20° to 60°S and from 50°W to 10°E. However, maximum lag separation shown later will be based on having an adequate number of pairs for the estimate of C.

2) The winter and summer seasons were divided into the three months June, July, and August, and December, January, and February, respectively. Monthly averages were calculated on a 4° × 4° grid for each of these months in the region of interest. In this way data from 1984, 1985, and 1986 were included in the calculation to form a long-term mean [Eq. (4)]. These means were then used to calculate anomalies for the buoys that wandered into any of the 4° × 4° boxes. These boxes then represented our effective Eulerian grid.

3) The product pairs were averaged over a month to estimate the correlations. The averaging procedure adopted for this process was one that weighted each monthly correlation by the number of pairs contributing to its calculation. This expression is given by

$$\hat{C}(\vec{r}, \tau) = \frac{\sum_{i=1}^{3} N_i C_i(\vec{r}, \tau)}{\sum_{i=1}^{3} N_i}, \quad (6)$$

where C_i refers to the monthly correlations from (5), and N_i is the number of pairs entering that calculation, thereby giving greatest weight to the best sampled estimate of C.

The two-dimensional correlations were smoothed in $\vec{r}$-space by averaging a given correlation with its eight neighbors weighted by the number of pairs contributing

to their calculation, thereby giving greatest weights to the best sampled estimate of C. This expression is given by:

$$\hat{C}_s(\vec{r}, \tau) = \frac{\sum_{\text{nearest neighbors}} N'\hat{C}(\vec{r}, \tau)}{\sum_{\text{nearest neighbors}} N'} \quad (7)$$

where $N' = \sum_{i=1}^{3} N_i$.

4) The determination of buoy separations and the methods used to resolve these separations into north–south components and east–west components deserve some discussion. There exists no scale preserving transformation such that the surface of a sphere may be projected onto a Euclidean (i.e., flat) grid. Thus while we can calculate the absolute distance between two points on a circle (via the arc length of the great circle defined by those two points) we can only find one component of this distance that is path independent. It was then our choice to take this one independent component as the buoy separation in the north/south direction and calculate its value via:

$$\Delta y = R \cdot \Delta\phi, \quad (8)$$

where R is the earth's radius and $\Delta\phi$ is the absolute value of the difference between latitudes for the data pair located at $\vec{x}$ and $\vec{x} + \vec{r}$.

The east/west separation was calculated by taking a path along the average latitude of the two buoys. The total east/west separation is then given by

$$\Delta x = R \cdot \cos(\bar{\phi}) \cdot \Delta\Theta, \quad (9)$$

where $\bar{\phi}$ is the average latitude of the two buoys and $\Delta\Theta$ is the difference of the longitudes of the two buoys. It will be important to keep in mind this approach when interpreting the estimates of the spatial scales of the TOGA drifter SLP, SST, and T fields.

In summary, determination of the characteristic spatial scales was estimated using a modified Eulerian correlation (5) with Lagrangian sampling under the assumption that averaging over 2000 pairs provides sufficient accuracy. In addition, it should be noted that the quasi-Eulerian correlations will be functions of spatial separations that are calculated using formulas (8) and (9).

c. *Results*

Two-dimensional correlations were calculated for observations that fell temporally within 24 hours of each other so $0 \leq \tau \leq 24$ hours and had spatial separations in the north/south and east/west directions that fell in the spatial bins 0 to 400 km, 400 to 800 km, etc. We found that the 24 hour and the 400 km bin widths gave adequate sampling to extract the relevant information on characteristic length scales.

TABLE 1. Decorrelation distances (km) from analysis of sea level pressure (SLP), sea surface temperature (SST) and surface air temperature (AT): X denotes decorrelation in east/west direction, and Y denotes decorrelation in north/south direction.

		Atlantic	Pacific
SLP:	Summer	$X = 2400$	$X = 1200$
		$Y = 2000$	$Y = 1600$
	Winter	$X = 2400$	$X = 2400$
		$Y = 2000$	$Y = 2800$
SST:	Summer	$X \geq 2800$	$X \geq 2800$
		$Y = 1600$	$Y = 1600$
	Winter	$X = 1600$	$X = 2800$
		$Y = 1200$	$Y = 1600$
AT:	Summer	$X = 1600$	$X = 2000$
		$Y = 1600$	$Y = 1600$
	Winter	$X = 2000$	$X = 1600$
		$Y = 1600$	$Y = 1600$

1) CHARACTERIZATION OF SEA LEVEL PRESSURE CORRELATIONS

The two-dimensional correlation function for the winter and summer TOGA SLP fields in both the South Pacific and South Atlantic oceans are shown in Fig. 7 (see also Trenberth 1985). What is immediately apparent from Fig. 7 is the increased scale lengths of the field in the wintertime especially in the Pacific. This increase in correlation is likely associated with the strengthening of the ultra long wave structure during the winter. This hypothesis finds further support by the appearance of a negative component in the east/west correlations at 3200 and 3600 km separations. Of further interest to us is the rather surprising fact that the two-dimensional correlation fields are fairly isotropic. This unexpected result may be due to the fact that our region of sampling was small relative to the Southern Hemisphere storm track.

Estimates of the SLP decorrelation distances are given in Table 1. These values are identified with the spatial lags at which the correlations in the first row and the first column of Fig. 7 obtained absolute values less than 0.05;* i.e., the first effective zero crossing of the correlation function. In the South Atlantic ocean, we see that, in spite of the increased length scale of the field in winter, the degree of isotropy does not change with season. In the South Pacific on the other hand, there is an elongation of both the east/west and north/south scales in the wintertime, in association with the development of the winter storm track (Trenberth 1982, 1984).

* The value of 0.05 represents a correlation of essentially zero based on the numbers of degrees of freedom in the datasets and the 95% confidence level. Other definitions of the decorrelation scale may give slightly different length estimates but not effect the qualitative aspects of the discussion.

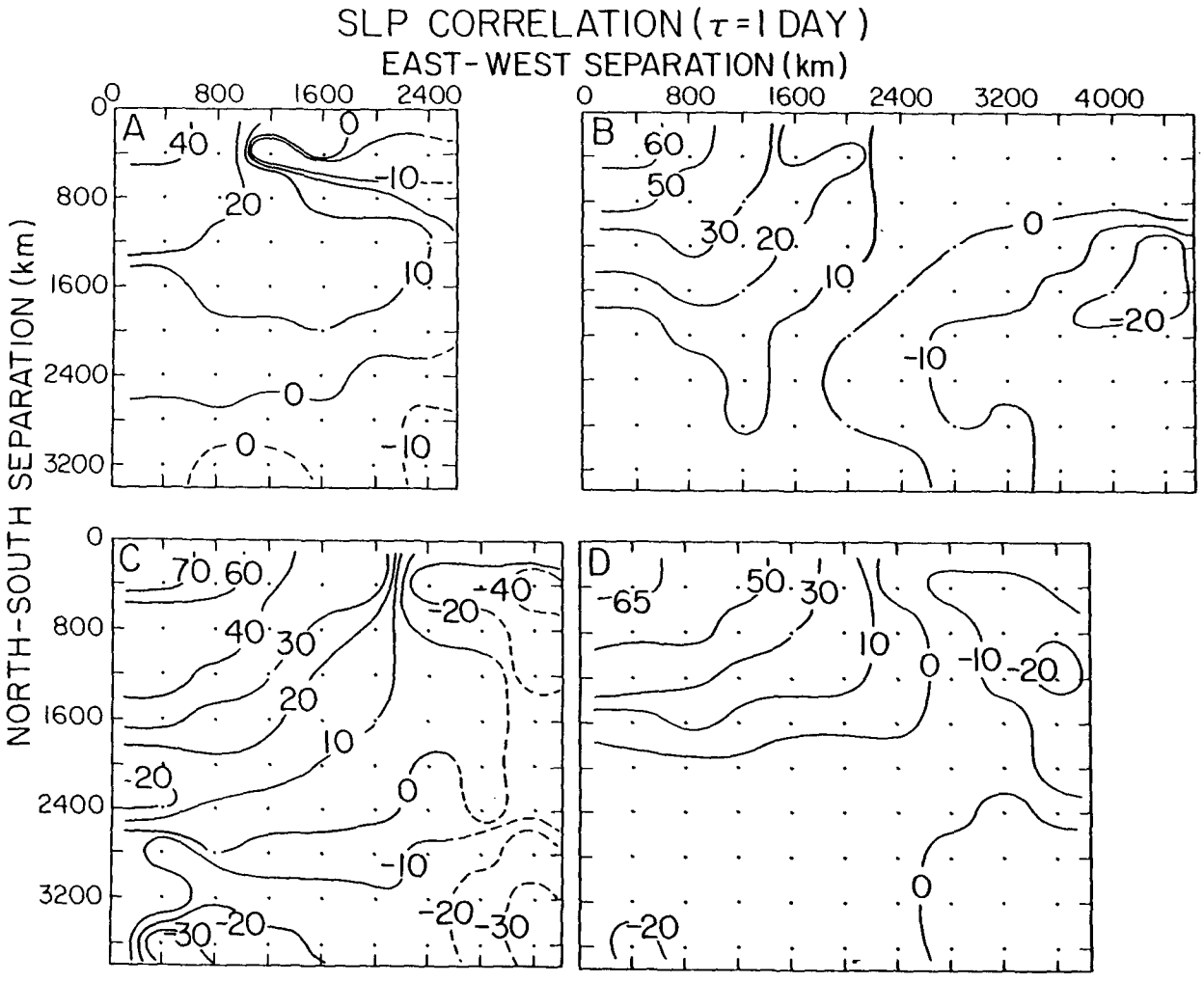

FIG. 7. Two dimensional correlation maps for $0 \leq T \leq 24$ hours for the daily SLP observations. Contours are in units of percent and the separation scale refers to the absolute value of the spatial lag. Maps (A) and (B) are the correlations for the South Pacific and South Atlantic summer while maps (C) and (D) are the correlation maps for the South Pacific and South Atlantic winter. Dashed contours represent poorly sampled regions of the field (<2000 pairs).

We repeated the above calculations as closely as we could using the NMC SLP analyses. In general, the results were much as noted above with one major exception. The analyzed data produced larger decorrelation length scales, presumably a result of the smoothing inherent in the analysis method. Indeed, estimates of the characteristic SLP length scales based solely on the analyses would be too large by some 20%–40% and so seriously underestimate the sampling requirements for a Southern Hemisphere SLP observing program.

2) CHARACTERIZATION OF SEA SURFACE TEMPERATURE CORRELATIONS

The SST data used in this phase of the study were nighttime data to avoid diurnal effects. The two dimensional correlation functions for the winter and summer SST fields in both the South Pacific and South Atlantic oceans are shown in Fig. 8. Decorrelation distances are tabulated in Table 1. We see that, past the 1600–2000 km separations, the correlation functions, in general, possess insignificant amplitude. Further, we may note that the Southern Hemisphere SST field seems to display an increased length scale during the summer months.

3) CHARACTERIZATION OF AIR TEMPERATURE CORRELATIONS

The two-dimensional correlation functions for the winter and summer TOGA nighttime air temperature fields (not shown) in both the South Atlantic and the South Pacific are given in Table 1. The conspicuous feature of these maps is the fact that there is very little

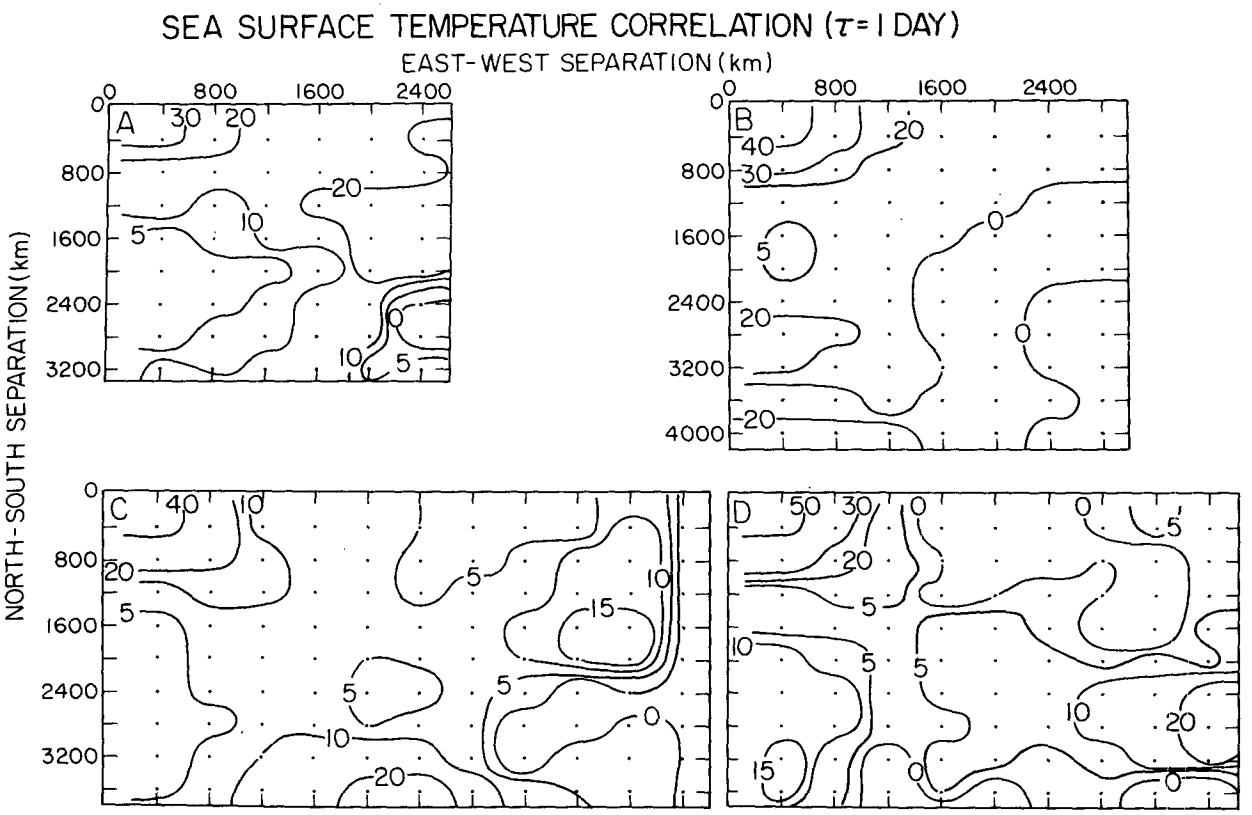

FIG. 8. Two-dimensional correlation maps for $0 \leq T \leq 24$ hours for the nighttime SST observations. Contours are in units of percent. Maps (A) and (B) are the correlations for the South Pacific and South Atlantic summer while maps (C) and (D) are the correlation maps for the South Pacific and South Atlantic winter.

seasonal change in the patterns of variability. In general, there is positive correlation up to 2000 km east–west separation and 2000 km north–south separation and then negative or low correlation past this point. Also of interest was the radial symmetry of these maps, a property we saw in both Figs. 7 and 8.

4. Summary and discussion

The first goal of this study was to obtain quality controlled data from the TOGA drifting buoy program for the period November 1984 to December 1986 and in doing so identify typical classes of errors. The motivation for this effort centered around the fact that these TOGA data had not, to date, been exploited by the scientific community and their quality was unknown. The comparisons of the TOGA drifter data with the COADS SST field, the Australian Weather Service and National Meteorological Center's SLP products from the Southern Hemisphere showed that in general, the drifter data agree with these other products. Since the drifter data go into these products in the first place one would expect a favorable comparison. In fact, the scatter in the SLP comparison was uncomfortably large. The reason(s) for this are unclear to us but it may have something to do with product quality and/or the impact the buoy data have (or have not had) on the analyses. The real utility of the drifter data could easily be determined by repeating several monthly analyses omitting the drifter data, and then compare the resulting monthly SLP field with the drifter data to see how much the buoys really helped. That effort is clearly beyond our capability.

A main goal of this study was to determine the characteristic spatial scales of the Southern Hemisphere SLP, SST, and T fields using the TOGA drifting buoy data. Our approach was to examine the two dimensional structure and correlation functions to determine decorrelation distances. We found that with up to a 24 hour time lag separation, one would get adequate sampling of the Southern Hemisphere climate fields with observations spaced 1500–2000 km apart. At 40°S these scales translate to buoy spacings of 30° longitude and 15°–20° of latitude. Using these numbers we can estimate (very crudely!) that a minimum of 30–40 fully functional buoys *deployed evenly* between 15° and 60°S would be able to adequately monitor the large scale structure of the SLP, SST, and T fields in the Southern Hemisphere. But clearly the buoy data, their advection rates, and their expected failure rates can be used to make a much more sophisticated estimate than we have made here.

The results of this study clearly suggest the TOGA drifter array is an invaluable element of the Southern Hemisphere observing system; indeed, an element that might be even more strongly exploited. The space/time distribution of data alone (Figs. 2 and 3) makes this point. Further, it appears the number of buoys currently in the array is close to optimum.

Acknowledgments. This work was supported by the TOGA Program under NOAA Grant NA87AA-D-AC083 and the National Science Foundation Climate Dynamics Program under Grants NSF ATM85-13713 and NSF ATM88-14571. We gratefully acknowledge useful comments on the manuscript especially by K. Trenberth, and also by R. Reynolds, S. Woodruff, R. Quayle, and two anonymous reviewers.

REFERENCES

Gilhousen, D., 1987: Quality control of drifting buoy data. Proc. COST-43 Conf., Brest, France.

Hamilton, G. D., 1986: National data buoy center programs. *Bull. Amer. Meteor. Soc.*, **67,** 411–415.

Reynolds, R., 1988: A real-time global sea surface temperature analysis. *J. Climate,* 75–86.

Tatarski, V. I., 1961: Wave propagation in a turbulent medium. Translated by R. Silverman, Dover Publishing, 285 pp.

Trenberth, K. E., 1981: Observed Southern Hemisphere eddy statistics at 500 mb: Frequency and spatial dependence. *J. Atmos. Sci.*, **38,** 2585–2605.

——, 1984: Interannual variability of the Southern Hemisphere circulation: Representativeness of the year of the global weather experiment. *Mon. Wea. Rev.*, **112,** 108–123.

——, 1985: Persistence of daily geopotential heights over the Southern Hemisphere. *Mon. Wea. Rev.*, **113,** 38–52.

——, and J. Olson, 1988: Evaluation of NMC Global Analyses: 1979–1987. NCAR Tech. Note, NCAR/TN-299+STR, 82 pp.